Journal of Luminescence 182 (2017) 196–199

Contents lists available at ScienceDirect

Journal of Luminescence

journal homepage: www.elsevier.com/locate/jlumin

The effects of indium aggregation in InGaN/GaN single and multiple quantum wells grown on nitrogen-polar GaN templates by a pulsed metalorganic chemical vapor deposition

Yu-Siang You [a], Shih-Wei Feng [a,*], Hsiang-Chen Wang [b], Jie Song [c], Jung Han [c]

[a] Department of Applied Physics, National University of Kaohsiung, No. 700, Kaohsiung University Rd., Nanzih District, Kaohsiung 81148, Taiwan, R.O.C
[b] Graduate Institute of Opto-Mechatronics, National Chung Cheng University, Chia-yi, Taiwan, R.O.C
[c] Department of Electrical Engineering, Yale University, New Haven, CT, USA

ARTICLE INFO

Article history:
Received 11 June 2016
Received in revised form
19 October 2016
Accepted 22 October 2016
Available online 26 October 2016

Keywords:
N-polar GaN
Pulse growth mode
Quantum well number
Indium aggregation

ABSTRACT

In this study, the effects of indium aggregation in InGaN/GaN single and multiple quantum wells (MQW) grown on nitrogen-polar GaN templates by a pulsed metalorganic chemical vapor deposition are investigated. With the pulsed growth mode, InGaN decomposition and indium aggregation lead to InGaN mounds, which forms localized states for trapping carriers. In the MQW sample, a higher density and larger size of InGaN mounds imply that an enhanced indium aggregation can improve luminescence efficiency.

© 2016 Elsevier B.V. All rights reserved.

1. Introduction

III-nitride semiconductors have been used for light-emitting diodes (LED), laser diodes, solar cells, and high electron mobility transistors (HEMT) [1–3]. These nitride devices are generally grown along the polar *c*-axis (*Ga*-polar), where the built-in polarization field decreases the overlap of the electron and hole wave functions and leads to quantum-confined Stark Effect (QCSE) [1–3]. At the same time, the advantage of reverse polarization field in *nitrogen (N)*-polar III-nitrides along the -*c*-axis [000$\underline{1}$] attracts more attention. By applying a larger forward bias in *N*-polar multiple quantum wells (MQW), a reduced QCSE increases overlap of electron and hole wave-function [4–7]. A stronger carrier localization and suppressed QCSE and electric field in an *N*-polar LED provide the advantages of efficient carrier relaxation and faster carrier recombination [4].

Currently, the luminescence efficiency of *N*-polar MQWs and LEDs is weaker than those of *Ga*-polar ones. Hexagonal hillocks on a rough surface are often observed in *N*-polar MQWs and LEDs [8–10]. An improved surface morphology and narrow spectral width can be obtained by growing *N*-polar GaN on misoriented sapphire, silicon carbide, and silicon substrates [11]. Also, it is reported that luminescence intensities of InGaN/GaN MQWs grown on *N*-polar GaN templates with a pulsed growth mode are better than those grown with a continuous growth method [12]. In pulsed growth mode, Ga and N sources are alternately injected into the reactor to alter the surface stoichiometry during the growth of InGaN/GaN MQWs grown on *N*-polar GaN templates, while trimethylindium (TMIn) was continuously injected at a constant flow rate. Using pulsed-mode creates a high density of hexagonal mounds with a higher InGaN growth rate and a higher indium composition around screw-type dislocations, resulting in improved luminescence properties. In general, the pulse durations of precursors are very important to influence the impurity incorporation rate in growing high quality Gas, lateral/vertical growth rate ratio in epitaxial lateral overgrowth, and the aspect ratio of GaN nanorods [12].

In this study, the effects of indium aggregation in InGaN/GaN single and multiple quantum wells grown on *N*-polar GaN templates by a pulsed metalorganic chemical vapor deposition are investigated by a high-resolution *x*-ray diffraction (XRD), atomic force microscopy (AFM), scanning electron microscope (SEM) and cathodoluminescence (CL) images, and photoluminescence (PL) measurements. With the pulsed growth mode, a higher density and larger size of InGaN mounds in the MQW sample imply that an enhanced indium aggregation can improve luminescence efficiency.

* Corresponding author.
E-mail address: swfeng@nuk.edu.tw (S.-W. Feng).

http://dx.doi.org/10.1016/j.jlumin.2016.10.039
0022-2313/© 2016 Elsevier B.V. All rights reserved.

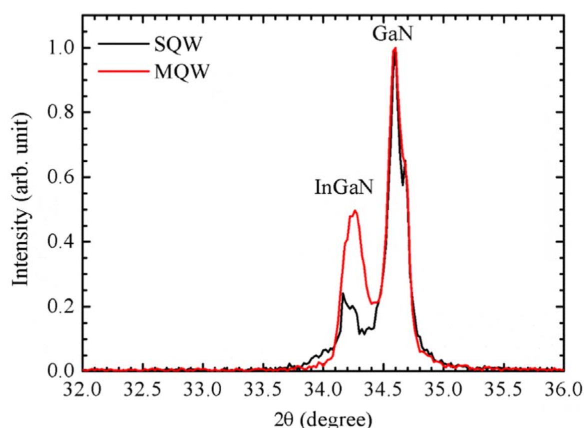

Fig. 1. XRD patterns for the InGaN/GaN SQW and MQW samples.

2. Experimental details

N-polar GaN used as templates were grown on *c*-plane $(000\bar{1})$ sapphire with 2° off-cut toward the *a*-axis. Sapphire was heated for nitridation in a mixture of ammonia (NH_3) (3 slm) and N_2 (4 slm) in a horizontal metalorganic chemical vapor deposition (MOCVD) reactor to 950 °C for 30 s. A 20 nm GaN nucleation layer was then grown on the nitridized sapphire at 600 °C in H_2 carrier gas, followed by 1 μm *N*-polar GaN being grown at 1055 °C and 100 mbar, with an NH_3 flow rate of 0.5 slm and a trimethylgallium (TMGa) flow of 66 μmol/min. During the growth, TMGa and NH_3 were used as Ga and N sources, respectively. The polarity of *N*-polar GaN templates was confirmed by convergent beam electron diffraction and wet etching in KOH solution. After growth of the *N*-polar GaN templates, the temperature was ramped down to 830 °C to grow the InGaN/GaN quantum well (QW) under N_2 carrier gas. TEGa, TMIn, and NH_3 were used as Ga, In, and N sources, respectively. During the growth of the QW, a pulsed-mode was employed to grow the InGaN QW, whereas continuous-mode was used to grow the GaN quantum barrier. The durations of TEGa "ON" and NH_3 "ON" are defined as $t_1(=3s)$ and $t_2(=5s)$, respectively. InGaN/GaN 1-QW (SQW) and 3-QW (MQW) samples were prepared. The details of the growth procedures are described in a previous study [12].

The structures of the SQW and MQW samples were investigated with a high-resolution XRD (Bede D1). The surface morphology was revealed by AFM (Park Systems, XE-70) with a non-contact mode using a silicon tip of curvature less than 10 nm. SEM and CL images were acquired with a Gatan monoCL3 spectrometer in a JEOL SEM system (model JSM 7000F) at room temperature (RT). The samples were placed in a cryostat for temperature-dependent PL measurement with the 325 nm line of a 55 mW He-Cd laser for excitation.

3. Results and discussion

Fig. 1 shows the XRD patterns for the two samples. The diffraction peaks corresponding to InGaN and GaN can be identified. The GaN diffraction peak is mainly from the barrier layers and GaN template. The side shoulder with a broad distribution below the GaN main peak is attributed to InGaN aggregation with various indium contents, sizes, and shapes in the quantum wells [13]. Because of the low miscibility of InN and GaN, indium aggregation and phase separation usually occur through spinodal decomposition in the quantum well [13]. The larger distribution of indium content, size, and shape in the MQW sample than that in the SQW one implies an apparent indium aggregation in the MQW.

Fig. 2(a) and (b) show the AFM images of the SQW and MQW samples, respectively. Hexagonal islands (called "mounds") with diameters of about a few hundred nanometers are observed on the surface. In transmission electron microscopy (TEM) images, the mounds seem to be formed at the apexes of dislocations with a screw-type component [12]. In and Ga atoms prefer to nucleate at the apexes of screw-type dislocations, where a higher InGaN growth rate and an enhanced indium incorporation occur. The surface roughnesses are 7.327 and 24.985 nm for the SQW and MQW samples, respectively. An apparent indium aggregation and a high density of mounds in the MQW increases the surface roughness.

Fig. 3 shows the SEM [(a) and (b)] and panchromatic CL [(c) and (d)] images for the corresponding SEM regions using the 11 kV excitation electron voltage for the SQW and MQW samples, respectively. InGaN mounds with diameters of about a few hundred nanometers are randomly distributed on the surface. A higher

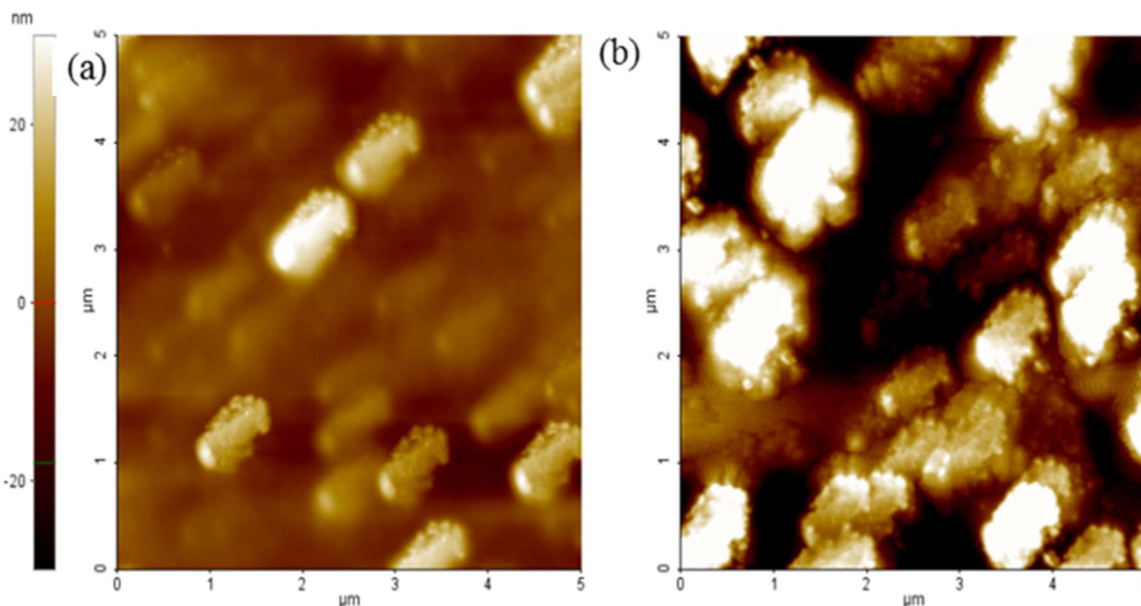

Fig. 2. AFM images (5 μm × 5 μm) of the InGaN/GaN (a) SQW (7.327 nm) and (b) MQW (24.985 nm) samples. Surface roughness of each sample is shown in the parentheses.

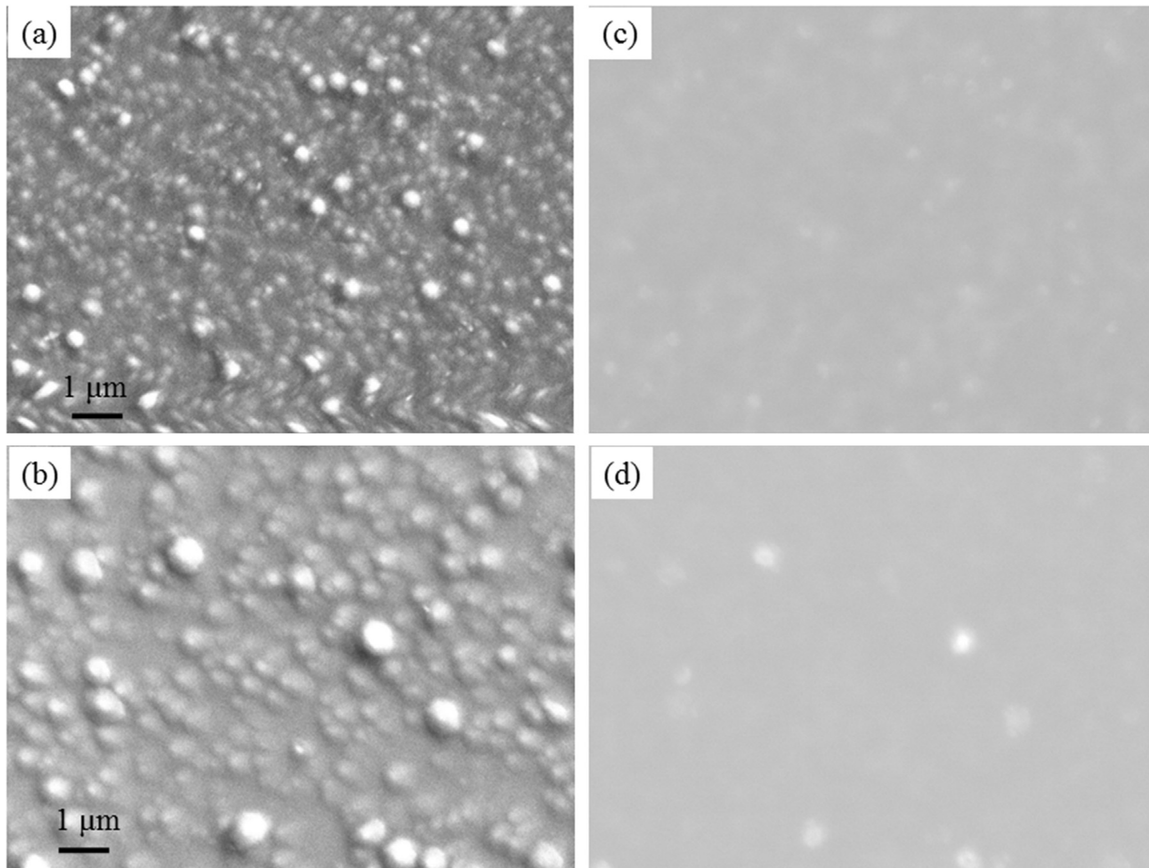

Fig. 3. SEM [(a) and (b)] and panchromatic CL [(c) and (d)] images for the corresponding SEM regions using the 11 kV excitation electron voltage for the InGaN/GaN SQW and MQW samples, respectively.

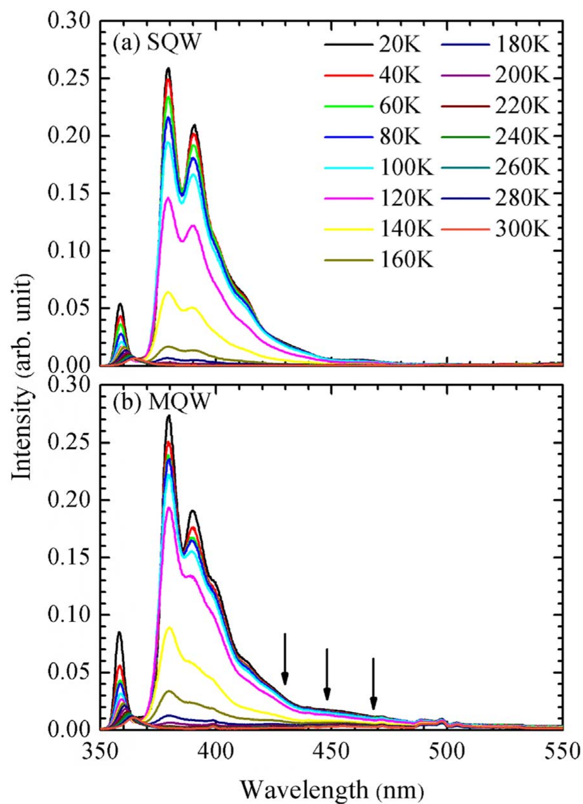

Fig. 4. PL spectra as a function of temperature for the InGaN/GaN (a) SQW and (b) MQW samples.

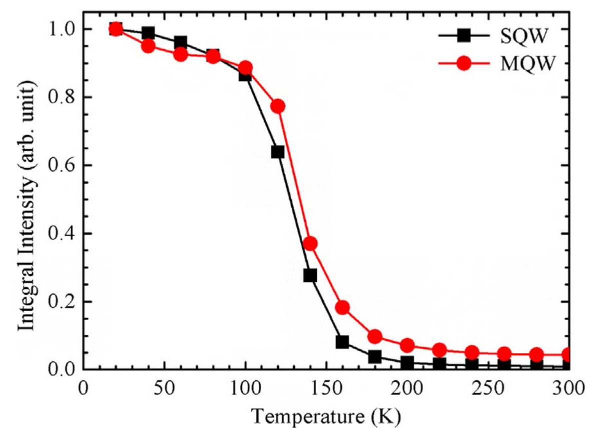

Fig. 5. Normalized integral PL intensity as a function of temperature for the InGaN/GaN SQW and MQW samples.

density and larger size of InGaN mounds in the MQW sample represent an apparent indium aggregation in the QWs. The light spots of a few hundred nanometers in CL image correspond to the indium-rich clusters [14]. It was claimed that the electroluminescence emissions come from the recombination of localized excitons in In-rich InGaN clusters [15–17]. For the MQW sample, more, larger, and brighter light spots reveal a better sample quality and InGaN/GaN MQWs show the advantage of improved luminescence efficiency. In TEM images, the first InGaN/GaN QW is uniformly grown on mounds and flat regions, while the upper InGaN/GaN MQWs are not [12]. In growing the upper MQWs, a high growth temperature has an annealing effect on the lower

QW. During annealing, spinodal decomposition may relax the strain energy built in the well layers. The up-hill diffusion gathers indium atoms toward centers and forms indium aggregations. Both enhanced carrier localization due to indium aggregation, and weaker internal electrical field due to thicker QWs contribute to an enhanced luminescence.

Fig. 4(a) and (b) show the PL spectra of the SQW and MQW samples respectively as a function of temperature. The SQW and MQW samples have three peaks: GaN emission band ~360 nm and two InGaN emission bands ~379 and ~390 nm. The dominant peak is ~379 nm (3.272 eV). A broader emission in the UV and visible spectral ranges, contributed from InGaN clusters with various indium contents, sizes, and shapes, is observed. Compared to the SQW sample, the slightly stronger UV peak ~379 nm (3.272 eV) and the enhanced luminescence in the 430–500 nm spectral range of the MQW sample can be attributed to an enhanced indium aggregation (InGaN clusters). At higher temperature(s), the enhanced nonradiative recombination decreases PL intensity. In addition, the normalized integral PL intensities in the 370–500 nm spectral range as a function temperature of the two samples are shown in Fig. 5. Due to nonradiative recombination, the integral PL intensities show a decreasing trend at higher temperature(s). When the temperature increases above 80 K, the stronger integral PL intensity for the MQW sample suggests that an enhanced indium aggregation is beneficial to luminescence efficiency.

4. Conclusion

In summary, we have shown the effects of indium aggregation in InGaN/GaN SQW and MQW samples grown on *N*-polar GaN templates by a pulsed growth mode. The pulsed growth mode enhances InGaN decomposition and indium aggregation such that InGaN mounds form spatial potential fluctuations and localized states for trapping carriers. A higher density and larger size of InGaN mounds in the MQW sample can trap more carriers and improve luminescence efficiency.

Acknowledgments

This research was supported by the Ministry of Science and Technology, Taiwan, under grants MOST 103–2112-M-390-002 and MOST 104–2112-M-390-002.

References

[1] E.F. Schubert, Light-Emitting Diodes, 2nd ed., Cambridge University Press, Cambridge, 2006.
[2] S.W. Feng, C.K. Yang, C.M. Lai, L.W. Tu, Q. Sun, J. Han, J. Phys. D: Appl. Phys. 44 (2011) 375103.
[3] S.W. Feng, C.M. Lai, C.H. Chen, W.C. Sun, L.W. Tu, J. Appl. Phys. 108 (2010) 93118.
[4] S.W. Feng, P.H. Liao, B. Leung, J. Han, F.W. Yang, H.C. Wang, J. Appl. Phys. 118 (2015) 043104.
[5] S. Keller, H. Li, M. Laurent, Y. Hu, N. Pfaff, J. Lu, D.F. Brown, N.A. Fichtenbaum, J. S. Speck, S.P. Denbaars, Semicond. Sci. Technol. 29 (2014) 113001.
[6] Q. Sun, Y.S. Cho, I.H. Lee, J. Han, B.H. Kong, H.K. Cho, Appl. Phys. Lett. 93 (2008) 131912.
[7] J. Song, G. Yuan, K. Xiong, B. Leung, J. Han, Cryst. Growth Des. 14 (2014) 2510.
[8] J.L. Weyher, A.R.A. Zauner, P.D. Brown, F. Karouta, A. Barcz, M. Wojdak, S. Porowski, Phys. Status Sol. (a) 176 (1999) 573.
[9] K. Kornitzer, T. Ebner, K. Thonke, R. Sauer, C. Kirchner, V. Schwegler, M. Kamp, M. Leszczynski, I. Grzegory, S. Porowski, Phys. Rev. B 60 (1999) 1471.
[10] M. Sumiya, K. Yoshimura, T. Ito, K. Ohtsuka, S. Fuke, K. Mizuno, M. Yoshimoto, H. Koinuma, A. Ohtomo, M. Kawasaki, J. Appl. Phys. 88 (2000) 1158.
[11] S. Fuke, H. Teshigawara, K. Kuwahara, Y. Takano, T. Ito, M. Yanagihara, K. Ohtsuka, J. Appl. Phys. 83 (1998) 764.
[12] J. Song, S.P. Chang, C. Zhang, T.C. Hsu, J. Han, ACS Appl. Mater. Interfaces 7 (2015) 273.
[13] Y.S. Lin, K.J. Ma, C. Hsu, S.W. Feng, Y.C. Cheng, C.C. Liao, C.C. Yang, C.C. Chou, C. M. Lee, J.I. Chyi, Appl. Phys. Lett. 77 (2000) 2988.
[14] S.W. Feng, L.W. Tu, J.I. Chyi, H.C. Wang, Thin Solid Films 517 (2008) 909.
[15] Y. Narukawa, Y. Kawakami, S. Fujita, S. Fujita, S. Nakamura, Phys. Rev. B 55 (1997) R1938.
[16] S.F. Chichibu, K. Wada, J. Müllhäuser, O. Brandt, K.H. Ploog, T. Mizutani, A. Setoguchi, R. Nakai, M. Sugiyama, H. Nakanishi, K. Korii, T. Deguchi, T. Sota, S. Nakamura, Appl. Phys. Lett. 76 (2000) 1671.
[17] Y. Narukawa, Y. Kawakami, S. Fujita, S. Nakamura, Phys. Rev. B 59 (1999) 10283.